

## VU Research Portal

### Localization of Fatty Acyl and Double Bond Positions in Phosphatidylcholines Using a Dual Stage CID Fragmentation Coupled with Ion Mobility Mass Spectrometry

Castro-Perez, J.; Roddy, T.P.; Nibbering, N.M.M.; Shah, V.; McLaren, D.G.; Previs, S.; Attygalle, A.B.; Herath, K.; Chen, Z.; Wang, S.P.; Mitnaul, L.; Hubbard, B.K.; Vreeken, R.J.; Johns, D.G.; Hankemeier, Th.

#### ***published in***

Journal of the American Society for Mass Spectrometry  
2011

#### ***DOI (link to publisher)***

[10.1007/s13361-011-0172-2](https://doi.org/10.1007/s13361-011-0172-2)

#### ***document version***

Publisher's PDF, also known as Version of record

[Link to publication in VU Research Portal](#)

#### ***citation for published version (APA)***

Castro-Perez, J., Roddy, T. P., Nibbering, N. M. M., Shah, V., McLaren, D. G., Previs, S., Attygalle, A. B., Herath, K., Chen, Z., Wang, S. P., Mitnaul, L., Hubbard, B. K., Vreeken, R. J., Johns, D. G., & Hankemeier, T. (2011). Localization of Fatty Acyl and Double Bond Positions in Phosphatidylcholines Using a Dual Stage CID Fragmentation Coupled with Ion Mobility Mass Spectrometry. *Journal of the American Society for Mass Spectrometry*, 22(9), 1552-1567. <https://doi.org/10.1007/s13361-011-0172-2>

#### **General rights**

Copyright and moral rights for the publications made accessible in the public portal are retained by the authors and/or other copyright owners and it is a condition of accessing publications that users recognise and abide by the legal requirements associated with these rights.

- Users may download and print one copy of any publication from the public portal for the purpose of private study or research.
- You may not further distribute the material or use it for any profit-making activity or commercial gain
- You may freely distribute the URL identifying the publication in the public portal ?

#### **Take down policy**

If you believe that this document breaches copyright please contact us providing details, and we will remove access to the work immediately and investigate your claim.

#### **E-mail address:**

[vuresearchportal.ub@vu.nl](mailto:vuresearchportal.ub@vu.nl)



## RESEARCH ARTICLE

# Localization of Fatty Acyl and Double Bond Positions in Phosphatidylcholines Using a Dual Stage CID Fragmentation Coupled with Ion Mobility Mass Spectrometry

Jose Castro-Perez,<sup>1,2</sup> Thomas P. Roddy,<sup>1</sup> Nico M. M. Nibbering,<sup>4</sup> Vinit Shah,<sup>1</sup> David G. McLaren,<sup>1</sup> Stephen Previs,<sup>1</sup> Athula B. Attygalle,<sup>5</sup> Kithsiri Herath,<sup>1</sup> Zhu Chen,<sup>1</sup> Sheng-Ping Wang,<sup>1</sup> Lyndon Mitnaul,<sup>1</sup> Brian K. Hubbard,<sup>1</sup> Rob J. Vreeken,<sup>2,3</sup> Douglas G. Johns,<sup>1</sup> Thomas Hankemeier<sup>2,3</sup>

<sup>1</sup>Department of Atherosclerosis Exploratory Biomarkers, Merck Research Laboratories, 126 E. Lincoln Ave, 80Y-2D7, Rahway, NJ 07065, USA

<sup>2</sup>Division of Analytical Biosciences, LACDR, Leiden University, Leiden, The Netherlands

<sup>3</sup>Netherlands Metabolomics Centre, LACDR, Leiden University, Leiden, The Netherlands

<sup>4</sup>LaserLab Amsterdam and Chemistry Department, Vrije Universiteit, Amsterdam, The Netherlands

<sup>5</sup>Center for Mass Spectrometry, Department of Chemistry, Chemical Biology and Biomedical Engineering, Stevens Institute of Technology, Hoboken, NJ, USA

### Abstract

A high content molecular fragmentation for the analysis of phosphatidylcholines (PC) was achieved utilizing a two-stage [trap (first generation fragmentation) and transfer (second generation fragmentation)] collision-induced dissociation (CID) in combination with travelling-wave ion mobility spectrometry (TWIMS). The novel aspects of this work reside in the fact that a TWIMS arrangement was used to obtain a high level structural information including location of fatty acyl substituents and double bonds for PCs in plasma, and the presence of alkali metal adduct ions such as  $[M+Li]^+$  was not required to obtain double bond positions. Elemental compositions for fragment ions were confirmed by accurate mass measurements. A very specific first generation fragment ion  $m/z$  577 (M-phosphoryl choline) from the PC [16:0/18:1 (9Z)] was produced, which by further CID generated acylium ions containing either the fatty acyl 16:0 ( $C_{15}H_{31}CO^+$ ,  $m/z$  239) or 18:1 (9Z) ( $C_{17}H_{33}CO^+$ ,  $m/z$  265) substituent. Subsequent water loss from these acylium ions was key in producing hydrocarbon fragment ions mainly from the  $\alpha$ -proximal position of the carbonyl group such as the hydrocarbon ion  $m/z$  67 ( $+H_2C-HC=CH-CH=CH_2$ ). Formation of these ions was of important significance for determining double bonds in the fatty acyl chains. In addition to this, and with the aid of  $^{13}C$  labeled lyso-phosphatidylcholine (LPC) 18:1 (9Z) in the  $\omega$ -position (methyl) TAP fragmentation produced the ion at  $m/z$  57.

**Electronic supplementary material** The online version of this article (doi:10.1007/s13361-011-0172-2) contains supplementary material, which is available to authorized users.

Correspondence to: Jose Castro-Perez; e-mail: jose\_castro-perez@merck.com

Received: 13 March 2011  
Revised: 15 May 2011  
Accepted: 17 May 2011  
Published online: 24 June 2011

And was proven to be derived from the  $\alpha$ -proximal (carboxylate) or distant  $\omega$ -position (methyl) in the LPC.

**Keywords:** Ion mobility, Mass spectrometry, Phospholipids, Time-of-flight, Fatty acids, Double bond position, CID fragmentation

---

## Introduction

Lipids play a very important role in human physiology and nutrition [1–5]. In this paper, we focus on the structural analysis of phosphatidylcholines (PC). This specific phospholipid subclass contains a polar head group and a glycerol backbone, which can be esterified by one (lysophosphatidylcholines (LPC)) or two (PC) different fatty acids occupying *sn*-1 or *sn*-2 positions [6, 7]. PCs represent the most abundant class of phospholipids in plasma and play a pivotal role directly or indirectly in several major enzymatic reactions occurring in circulation and in tissues. For example, PCs can be hydrolyzed by endothelial lipase (EL) [8] to generate LPCs, which can turn on signaling pathways in many tissues upon absorption. Since the position of double bonds bears an impact on the LPCs signaling properties, it is of high interest to locate the position of the double bond in the fatty acyl chains of PCs. In addition, certain enzymes have a prevalence to select different fatty acyl compositions in the PC. For example, lecithin: cholesterol acyltransferase (LCAT) in circulation favors fatty acyl 18:1 and 18:2 over 20:4 and 22:6 at the *sn*-2 position of PC in human beings [9].

Positional determination of fatty acyl groups in PCs and subsequent location of the double bond is a laborious and complex process. In the past, location of the fatty acyl group in PCs has been achieved either by enzymatic means in combination with mass spectrometry, or solely relying on mass spectrometry. Enzymatic assays involved digestions of PCs using phospholipase A1 or A2. As a result, specific cleavage by hydrolysis takes place for either the *sn*-1 or *sn*-2 position.

Over the years, there has been a variety of different mass analyzers [10], which have been applied to lipid analysis ranging from sector instruments, tandem quadrupoles, time-of-flight mass spectrometers, Orbitrap, Fourier transform-ion cyclotron resonance (FT-ICR), and linear ion traps all using a variety of different ionization techniques, including electron ionization (EI), fast atom bombardment (FAB), matrix-assisted laser desorption ionization (MALDI) [11], and electrospray (ESI) ionization. The early pioneering work of Gross and co-workers paved the path in the research of lipid fragmentation mechanisms and double bond localization by the use of high-energy collision-induced dissociation of the carboxylate anions of free fatty acids, generated by FAB and without a derivatization step [12–14]. Their research showed that by high-energy collision-induced charge-remote fragmentation the position of the double bond

in a mono-unsaturated fatty acid could be determined. This method worked also for poly-unsaturated fatty acids, although the data interpretation step was rather complex for locating the double bonds.

As electrospray became more widely adopted, Murphy et al. [15] and Kerwin et al. [16] implemented this ionization technique for the analysis of PCs using either positive or negative ion electrospray. In the positive ion electrospray mode and in the absence of alkali metal adduct ions such as lithium (which is introduced post-column), PCs are primarily ionized as  $[M+H]^+$  ions. Under these conditions, low-energy collision induced dissociation (CID) mainly yields the favorable loss of the phosphocholine head group, with little or no information about the fatty acyl groups or double bond position [17, 18]. In negative ion mode PCs are detected in an ammonium acetate buffered methanol solution as  $[M+CH_3COO]^-$  or  $[M-CH_3]^-$ , the latter being due to loss of methyl acetate formed via abstraction of a methyl cation from the quaternary ammonium group by the acetate anion. The  $[M-CH_3]^-$  ions do generate upon low-energy CID relatively low abundant  $R_1COO^-$  and  $R_2COO^-$  ions from which could be difficult to generate by charge-remote fragmentation sufficiently abundant fragment ions to locate their double bond position.

The use of alkali metal adducts and, more specifically, lithium adducts to generate fragmentation of fatty acyl chains for localization of double bonds has been extensively utilized in electrospray ionization mode. For instance, Hsu et al. [19, 20] has comprehensively studied the fragmentation mechanism of PCs showing that it is possible to obtain fatty acyl information by low-energy CID using a tandem quadrupole. With respect to the utilization of a multi-stage CID approach for the localization of double bonds in the fatty acyl chains, Bryant et al. [21] demonstrated that it was possible to obtain FAB-MS<sup>3</sup> fragmentation with a four sector MS instrument for the analysis of phosphatidylcholines present in a human immunodeficiency virus. In spite of the fact that at the time this was an innovative approach, the sensitivity obtained from this instrument arrangement is relatively low compared with other mass spectrometers currently available, such as tandem quadrupoles or time-of-flight mass spectrometers. MS<sup>n</sup> experiments involving the use of lithiated adducts have also been studied using linear ion trap mass spectrometers as described by Hsu et al. [22]. Different phospholipid classes were analyzed using the lithiated approach yielding detection as  $[M+Li]^+$ ,  $[M-H+2Li]^+$ , and  $[M-2H+3Li]^+$  ions. Hydrocarbon fragment ions from this approach are generated from the fatty acyl chains,

forming allylic and vinylic fragment ions. In some cases (phosphatidic acid (PA), phosphatidylserine (PS), and lysophospholipids), further multi-stage fragmentation up to MS<sup>5</sup> is required to obtain double bond information. Consequently, fragment ions belonging to the fatty acyl moiety result in yielding very low ion abundances, thus making interpretation challenging.

An alternative technique involving the use of ozone gas to oxidize the carbon–carbon double bond/s in fatty acids and provide real-time double bond analysis in the MS has been previously investigated by Thomas et al. [23, 24]. There are different ways to introduce this reactive gas into the mass spectrometer. It can be introduced directly in the electrospray ionization source, which entails the use of oxygen as the nebulization gas and using a high voltage on the capillary producing a corona discharge to generate ozone gas. An alternative method involves the direct supply of ozone to the ion source. This latter approach permits for a superior management of ozone gas introduced in the ionization chamber. Fragmentation information in this fashion arising from “ozone induced dissociation (OzID)” is very complicated, especially in complex lipid mixtures containing isobaric lipids, which may contain similar fragment ions. Recently, introduction of ozone post-ionization was thoroughly documented using an ion trap mass analyzer [25]. The most immediate advantage here is that complex mixtures can be handled in a much better fashion by mass selection of specific lipids and subsequent MS<sup>n</sup> experiments. Although this technique, so-called “ozonolysis,” is extremely useful, there are health hazards involved in the use of ozone gas in the laboratory, thereby requiring constant monitoring of its level.

As technology evolved in mass spectrometry, ion mobility mass spectrometry (IMS) has become a key component in proteomic and lipidomic analysis [26–34]. IMS has the capability of separating ions based on the size, collisional cross sections, and charge state. Monitoring these ions under the influence of a gas, typically nitrogen, in the presence of an electric field produces different mobility times in the drift tube. Hence, this offers an additional level of selectivity on top of *m/z*, retention times and peak intensity values. Ion mobility has been used as a tool to achieve a better understanding of the stoichiometry of large molecular weight proteins in the gas phase [35–37]. Yet, this type of configuration can be employed as well in studying small molecules as demonstrated by the IMS separation of regional isomers [38, 39].

In this report, we describe the use of a traveling-wave ion mobility spectrometry procedure (TWIMS), which enables the identification of the fatty acid substituents at *sn*-1 or *sn*-2 positions of the PC as well as the location of double bonds in the fatty acid chains. This TWIMS device [40] consists of an ion mobility drift tube positioned between a quadrupole mass analyzer and an orthogonal time-of-flight mass spectrometer. Another important aspect of this study is that up to now there

has been no report using LC/MS in electrospray positive ion mode without any derivatization agent or adducts that has been able to localize double bonds in the fatty acyl substituents of PCs.

## Material and Methods

### *Chemicals and Reagents*

Lipid standards were obtained from Avanti Polar Lipids (AL, USA). PC (16:0/14:0); PC(16:0/18:0); PC[16:0/18:1(9Z)]; PC[16:0/18:2(9Z,12Z)]; PC [16:0/20:4(5Z,8Z,11Z,14Z)]; PC [16:0/22:6(4Z,7Z,10Z,13Z,16Z,19Z)]; LPC (18:0); LPC [18:1 (9Z)] were prepared as stock solutions in dichloromethane (1mg/mL) and stored at –20°C until further analysis. Labeled lipid standards, PC[16:0/<sup>13</sup>C<sub>1</sub> labeled at ω methyl position 18:1(9Z)]; LPC [<sup>13</sup>C<sub>1</sub> labeled at ω methyl 18:1(9Z)] were purchased from Cambridge Isotec (97% purity) (MA, USA). These standards were also prepared as stock solutions in dichloromethane (1mg/mL) and stored at –20°C. A solution of leucine enkephalin (Sigma Aldrich, St. Louis, MO, USA) at a concentration of 2ng/μL in 50/50 vol/vol acetonitrile/water (0.1% formic acid) was used for lock mass correction.

### *Biological Sample Preparation*

All animal protocols were reviewed and approved by the Merck Research Laboratories Institutional Animal Care and Use Committee (Rahway, NJ, USA). Male C57Bl/6 mice (Taconic Farms, Inc., Germantown, NY, USA) were maintained on a regular chow diet. Mice were tail bled and the plasma was collected in EDTA tubes with lipase inhibitors added. In addition to this, human and rhesus macaque plasma samples (Bioreclamation, SC, USA) were also used. An aliquot of plasma (20μL) was extracted by the Bligh and Dyer method [41].

### *Liquid Interface and Ion Mobility TOF Mass Spectrometric Conditions*

Two types of liquid introduction systems were utilized for mass spectrometric experiments on a SYNAPT G2 HDMS (Waters MS Technologies, Manchester, UK). Synthetic lipid samples were examined by flow injection analysis (FIA), using a robotic chip-based nano-electrospray delivery device (Advion Nanomate, NY, USA). Samples were introduced to the mass spectrometer by infusing through a 5-μm nozzle. A voltage of +1.5 kV was applied to the conductive disposable sample pick-up tip. For standard lipid samples (concentration 100ng/μL), 5-μL aliquots were injected using a new tip for each delivery, to minimize the risk of sample contamination. Data was collected for 10 min per sample.

For the analysis of plasma samples, an Acquity UPLC (Waters, MA, USA), a high-pressure solvent delivery system was coupled to the mass spectrometer; same chromato-

graphic conditions were used as described in previous work [42]. Electrospray (ESI) ionization mass spectra were recorded under positive ion generating conditions while maintaining the capillary, extraction cone, and cone voltages at +2 kV, +4 V, and +30 V respectively for-LC related experiments. The desolvation nitrogen gas was used at a flow rate of 700 L/h, the source and desolvation temperatures were set at 120 and 450°C respectively. Mass spectra ( $m/z$  50–1200) were acquired at a resolving power of 25,000 [full width half height mass resolution (FWHM)]. Leucine enkephalin was used as the lockmass for all the experiments described herein. The lockmass was introduced automatically with a built-in solvent delivery system at a flow rate of 10  $\mu$ L/min, and acquired for 0.3 s; this event was repeated every 10 seconds in a separate acquisition channel. Lock-mass corrections were applied in a post-processing manner.

### *Ion Mobility Time-Aligned Parallel (TAP) Fragmentation Experimental Conditions*

For fragmentation experiments the instrument was set up in a mode called time-aligned parallel fragmentation (TAP), in which both collision cells (trap and transfer) were maintained at a collision energy setting of 35 eV. The collision gas utilized was argon at a pressure of  $9.11 \times 10^{-3}$  mbar. Under this mode of operation, ions of interest were selected in the quadrupole region Q1 at a resolution of 1 Da to allow only ions of one  $m/z$  ratio to pass through. Ions isolated in this way were subjected to subsequent fragmentation in the “trap” region of the IMS device. These first generation fragment ions entered the helium cell region that was operated at 150 mL/min; the main function of the helium cell was to reduce the internal energy of ions and minimize further fragmentation. First generation daughter ions then entered the IMS cell, held under 80 mL/min flow of nitrogen, to be separated according to their charge,  $m/z$ , and collisional cross section areas. As the separated ions exited the IMS cell, they were subjected to a second fragmentation event where each ion produced a series of second generation grand-daughter ions. Each spectrum produced in this way corresponds to a specific drift time that can be aligned with a first generation daughter ion or mixture of ions. The trap T-wave, IMS T-wave, and the transfer T-wave all carried different wave velocities; these were 314, 652, and 190 m/s respectively. The total cycle span for a TAP fragmentation experiment was 10.75 ms. Each total fragmentation including IMS separation adds up to 200 IMS scans or bins, thus each scan accounting for 53.75  $\mu$ s, so that over the course of an LC run or FIA a large number of ion mobility scans can be attained.

### *TWIMS Calibration Procedure*

The movement of ions through the T-wave mobility device is somewhat different from that in more conventional drift

tubes that use a constant electric field. Thus, it is necessary to calibrate the TWIMS device with a calibration mixture of known collision cross sectional (CCS) areas as reference markers. For the calibration of the TWIMS device, a mixture of poly-DL-alanine (Sigma-Aldrich) (1 mg/mL) in 50/50 vol/vol methanol/water was infused for a total of 5 min to collect sufficient data points for the calibration. Only singly charged species of the calibrant ions were processed for the calibration curve. The drift time ( $t_c$ ) was plotted against normalized cross section and a linear trend line ( $y = ax + b$ ) was constructed. The linear calibration curve ( $r^2 = 0.9908$ ; Figure S-1) obtained in this way was then used to calculate collision cross section areas ( $\text{\AA}^2$ ) of other ions subjected to mobility in the T-Wave cell. The same calibration line was applied to all measurements by maintaining all IMS parameters constant throughout the experiments.

All the data generated in these experiments was processed by a special software algorithm designed by the manufacturer (DriftScope 2.1) as part of the MassLynx 4.1 software package. The main function of DriftScope was to deconvolute IMS data from a multidimensional format (retention time,  $m/z$ , peak intensity, and drift time) to a two-dimensional display (drift time and  $m/z$ ). In other words, the data was first deconvoluted in the DriftScope and then exported to MassLynx for further data processing.

### *Lipid Nomenclature*

Throughout this study, the lipid nomenclature utilized was the same as cited by LIPIDMAPS (<http://www.lipidmaps.org>) following the article by Fahy et al. [6]

## **Results and Discussion**

### *LC-IMS/TOF-MS Plasma Lipid Analysis*

Data obtained from an LC-IMS/TOF-MS analysis of mouse plasma are illustrated in Figure 1a. Although the presence of a large number of components in the plasma mixture is evident from the reverse-phase LC-IMS/TOF-MS profile obtained (Figure 1a, top), the occurrence of three major different drift-time regions (Figure 1a, bottom, bright yellow patches) indicate the existence of three different clusters of lipid classes in the lipid plasma extract. Even though recording of TOF spectra in conjunction with IMS has some merit, enhanced structural information can be generated if the two collision cells are operated in tandem with the IMS device. This procedure named TAP protocol is the main focus of the research reported here. For example, the ion  $m/z$  760.6 from one of the major lipids of interest PC [16:0/18:1 (9Z)] in plasma that eluted at retention time 6.0 min was selected with the quadrupole mass filter (1-Da wide isolation window) and subjected to fragmentation in the first collision cell (Figure 1b); a packet of daughter ions produced in the trap region were subjected to ion mobility separation followed by secondary fragmentation



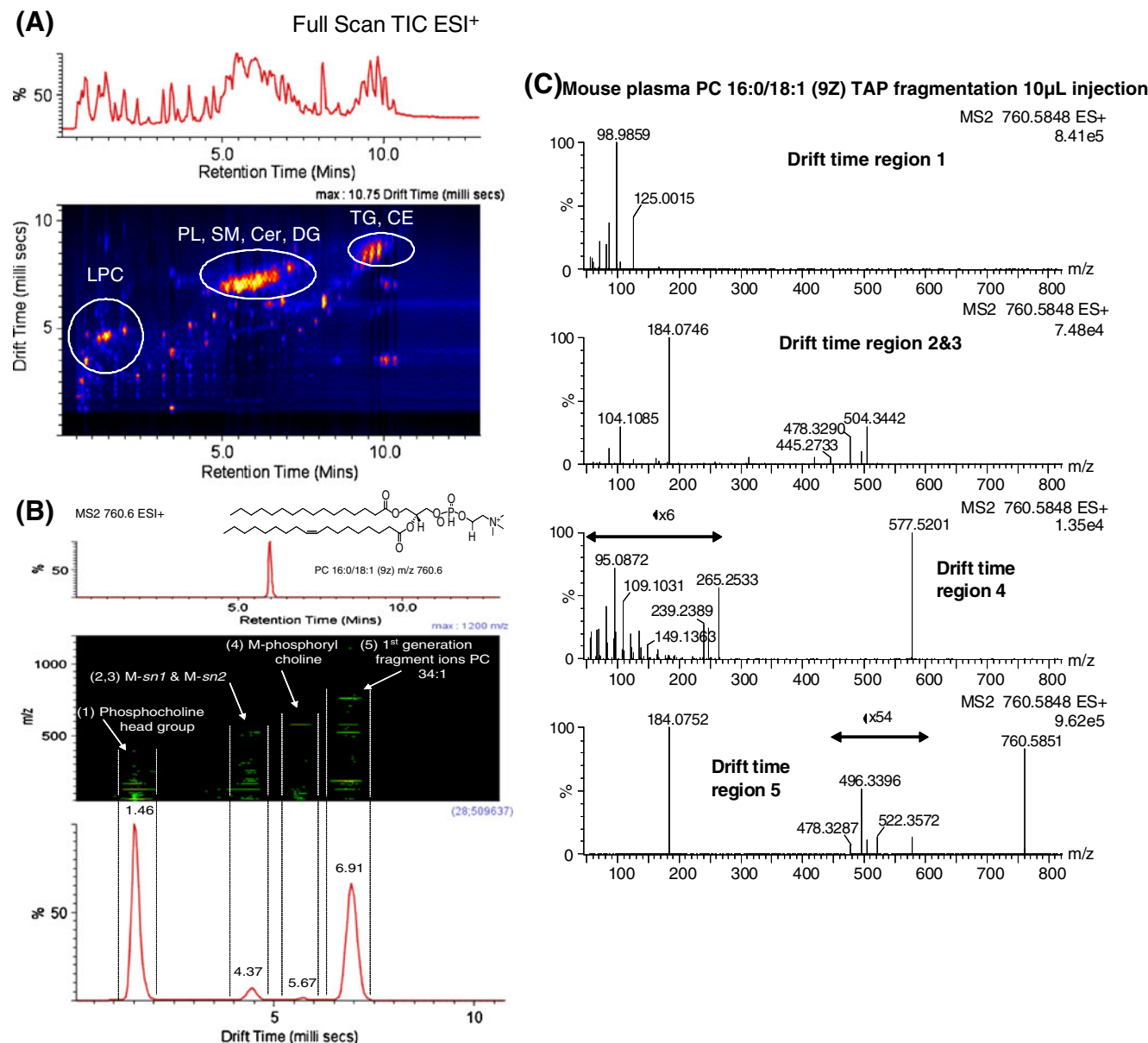


**Figure 1.** LC/IMS-TOF MS and TAP lipid analysis in extracted mouse plasma. **(A)** A chromatogram recorded by acquiring  $m/z$  50–1200 mass range (top) and ion mobility data (bottom) for 13.0 min on an LC/IMS-TOF instrument from an extracted mouse plasma sample (LPC=lyso phosphatidylcholine; PL=phospholipid; SM=sphingomyelins; Cer=ceramides; DG=diacylglycerides; TG=triacylglycerides, CE=cholesterol ester) **(B)** TAP data from the  $m/z$  760.6 ion, for PC 16:0/18:1 (9Z) from an extracted mouse plasma sample, isolated in Q1 and then subjected to fragmentation. **(C)** TAP fragmentation spectra corresponding to each of the drift time regions in the driftogram shown in panel **(B)**

in the transfer region, resulting in a driftogram containing the different drift regions for each of the first generation and second generation fragment ions generated in this arrangement (Figure 1b). Figure 1c shows in detail the spectra contained in each of the drift time regions generated by TAP fragmentation from mouse plasma; the peak centered at 1.46 ms represents the  $m/z$  184 ion derived from the phosphocholine head group. The drift region centered around 4.37 ms represents a composite of

several ions that originated from the loss of the acyl chains ( $M - sn-1$  and  $M - sn-2$ ). The drift time region at 5.67 ms corresponds to the M-phosphoryl choline fragment ion. Finally, the drift time region centered at 6.91 ms represents the first generation fragment ions of precursor [PC (16:0/18:1 (9Z))]. The sensitivity obtained from this LC on-line IMS-TOF experiment was adequate. Even though the hydrocarbon fragment ions generated in drift time region 4 were of low abundance, it was possible

to detect them without the need of fraction collection of the peak followed by flow injection analysis. To determine whether low PCs levels may affect our ability to obtain a good degree of fragmentation information for region 4 in the driftogram, a 1  $\mu$ L injection of the extracted plasma sample was carried out. The data shown in Figure S-2 clearly depicts the fact that we were able to detect with a good ion count the lower injection volume for the same drift time region 4.

In order to confirm the fragmentation content of the ions present in the trap region in detail, a sample of synthetic standard PC 16:0/18:1 (9Z) was infused by flow injection and product-ion spectra corresponding to each region were obtained. Typically, CID spectra of PCs show only a very intense peak at  $m/z$  184, which corresponds to the phosphocholine head group, and provides little information on the fatty acyl chains at the *sn*-1 or *sn*-2 positions. With the use of TAP fragmentation in combination with ion mobility, enhanced structural information on these ions can be obtained. All fragmentation reported

herein was a direct result of charge-induced fragmentation (CIF). Stable isotope  $^{13}\text{C}$  labeling of the terminal carbon at position 18 of the *sn*-2 fatty acyl chain was used for the PC and LPC, not only to guide us in the data interpretation for the localization of fatty acyl and double bond positions, but also to find out whether fragmentation originated in the distant or proximal carbon position from the carbonyl group. This will be discussed later in more detail.

### Loss of the Phosphoryl Choline Head Group

Use of a synthetic standard to confirm the TAP fragmentation results in Figure 1c was important in this study. Figure 2a–d give the corresponding spectra for all the driftogram regions shown in Figure 1c using the synthetic standard. The  $m/z$  577.5201 (+0.9 ppm calculated for  $\text{C}_{37}\text{H}_{69}\text{O}_4$ ) ion represented by the peak at 5.67 ms in Figure 1c, produced the product ion spectrum observed in Figure 2c. The  $m/z$  577.5 ion in fact corresponds to the loss

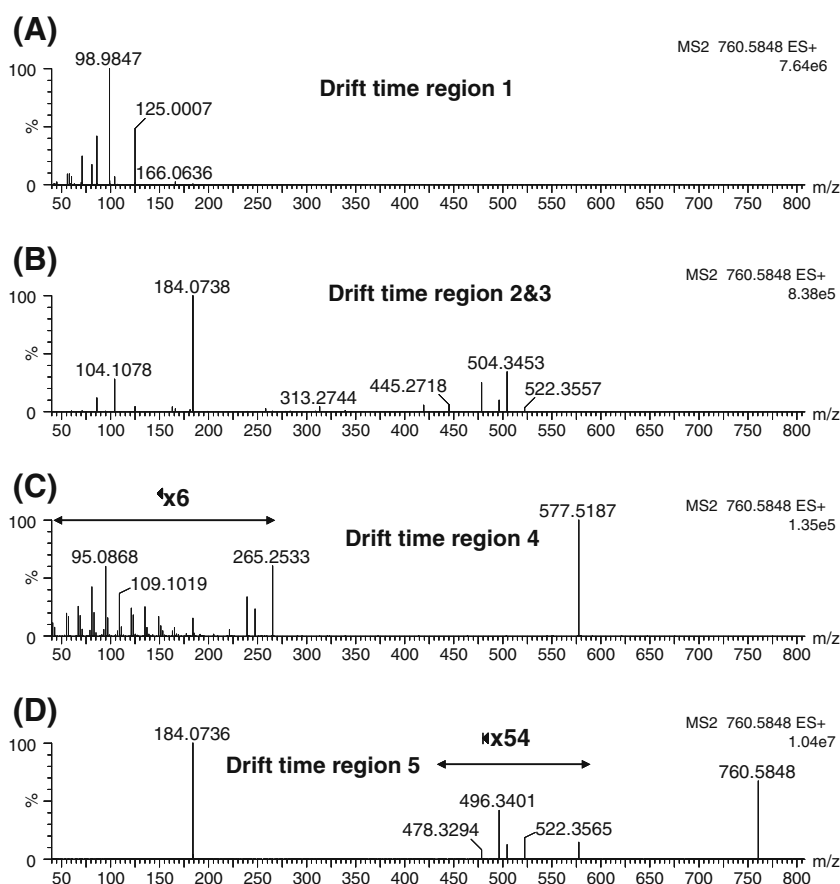


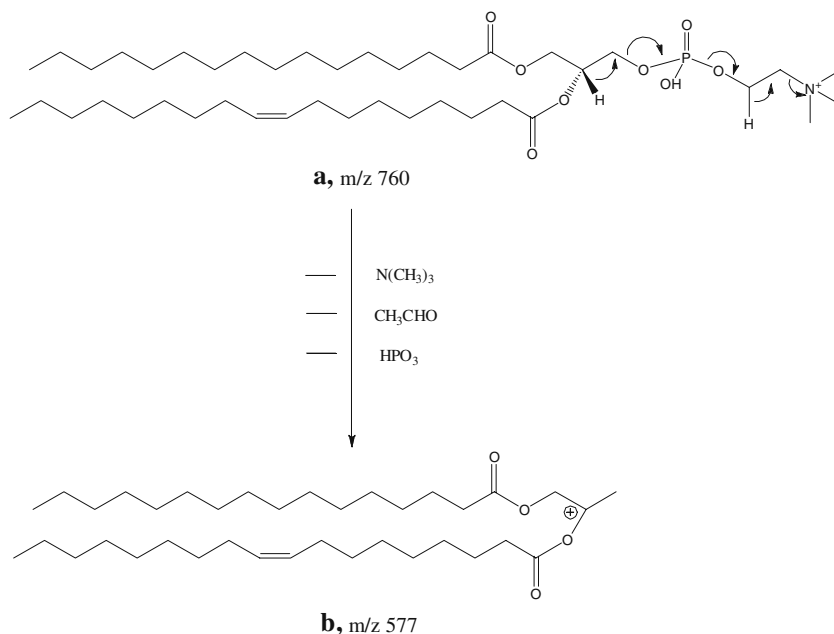
**Figure 2.** Synthetic flow injection analysis standard  $m/z$  760.5848 [PC 16:0/18:1 (9Z)] showing collision induced dissociation mass spectra for ions arising from the TAP experiment with drift times corresponding to 1.45 (A), 4.37 (B), 5.67 (C), and 6.91 ms. (A) Drift time region 1; phosphocholine head group (transfer fragments). (B) Drift time region 2 and 3; M-*sn*1 and M-*sn*2 (transfer fragments). (C) Drift time region 4; M-phosphoryl choline (transfer fragments). (D) Drift time region 5; first generation fragment ions from PC 16:0/18:1 (9Z) (trap fragments)

of the phosphoryl choline head group from the precursor ion  $m/z$  760.5; this particular fragmentation step is not energetically favorable. This is supported by the observation that the relative peak intensity of the  $m/z$  577 ion driftogram is significantly smaller than those of the other peaks in the driftogram (Figure 1b). The subsequent fragments from this ion resulted from a secondary fragmentation process in the transfer region being derived from the parent ion. The generation of the  $m/z$  577 ion is postulated in Scheme 1, sequence **a**→**b**. Presumably, this fragmentation step arises from CIF in which heterolytic cleavage of the C–N bond in ion **a** is successively accompanied by a concomitant 1,2-hydride shift and loss of  $\text{CH}_3\text{CO}$ , followed by loss of  $\text{HPO}_3$  and again a concomitant 1,2-hydride shift to give ion **b** with  $m/z$  577. The two 1,2-hydride shifts during this fragmentation avoid the formation of primary carbenium ion centers, which theoretically are known not to correspond to energy minima. Without the use of lithiated PC adducts, there is little evidence in the literature for this particular fragmentation process; Trimpin et al. [43] have indicated the occurrence of this fragment ion without support from accurate mass measurements. Furthermore, the IMS configuration used in that work was different from the one applied in the present research. Table S-1 shows all the different fragment ions generated in each of the drift time regions together with their accurate mass. All first and second generation fragment ion accurate mass measurements gave a total RMS error of 1.56 ppm, which is very acceptable in view of the fact that such measurements by use of IMS TOF have not been reported earlier. From Table S-1, it can be noted that drift fragmentation region 4 contains fragment ions that for the major part may contain 0, 1, 2, or 3

double bonds. These ions are generated from CIF events, which will be discussed below.

### Location of the Fatty Acyl Substituent Positions

For the determination of the position of the fatty acyl chain in the *sn*-1 or *sn*-2 positions,  $m/z$  760.5 corresponding to PC 16:0/18:1 (9Z) was selected in the quadrupole region (Q1). This was followed by CID fragmentation in the trap region, and drift times belonging to regions 2 and 3 were used (see Figure 3). Figure 3a shows in detail the results from three different biological matrices (rhesus, mouse, and human plasma) injected on the LC column and detected by the IMS-CID-TOF. In all cases, the data shows that *sn*-2 is preferentially fragmented over *sn*-1. This was confirmed by the use of synthetic standards, where the FA 16:0 constituent was either in the *sn*-1 or *sn*-2 positions [PC 16:0/18:1 (9Z) or PC 18:1 (9Z)/16:0] and PC 16:0/18:1 (9Z)  $^{13}\text{C}_1$  ( $\omega$  in methyl position). In Figure 3b, it can be observed that if the same synthetic standard [PC 16:0/18:1 (9Z)] is used as in the plasma samples, the same fragmentation pattern is detected. In contrast to this, if the FA 16:0 substituent is now in the *sn*-2 position [PC 18:1/ 16:0 (9Z)], the opposite is observed. One interesting observation in comparison with the plasma samples for the isomeric synthetic standards and especially for PC 16:0/18:1 (9Z) is that it seemed there was a discrepancy between the ratio corresponding to the loss of *sn*-1 ( $m/z$  522) relative to *sn*-2 ( $m/z$  496); ~26% for the human plasma and ~38% for the synthetic standard (% is calculated as % spectral intensity by combining 10 consecutive scans). Therefore, it is possible that the synthetic standard contains isomeric impurities of ~12% and one could assume that the plasma samples have no isomeric



Scheme 1. Proposed mechanism for the formation of M-phosphoryl choline ion  $m/z$  577 arising from TAP charge-induced fragmentation of PC 16:0/18:1 (9Z)



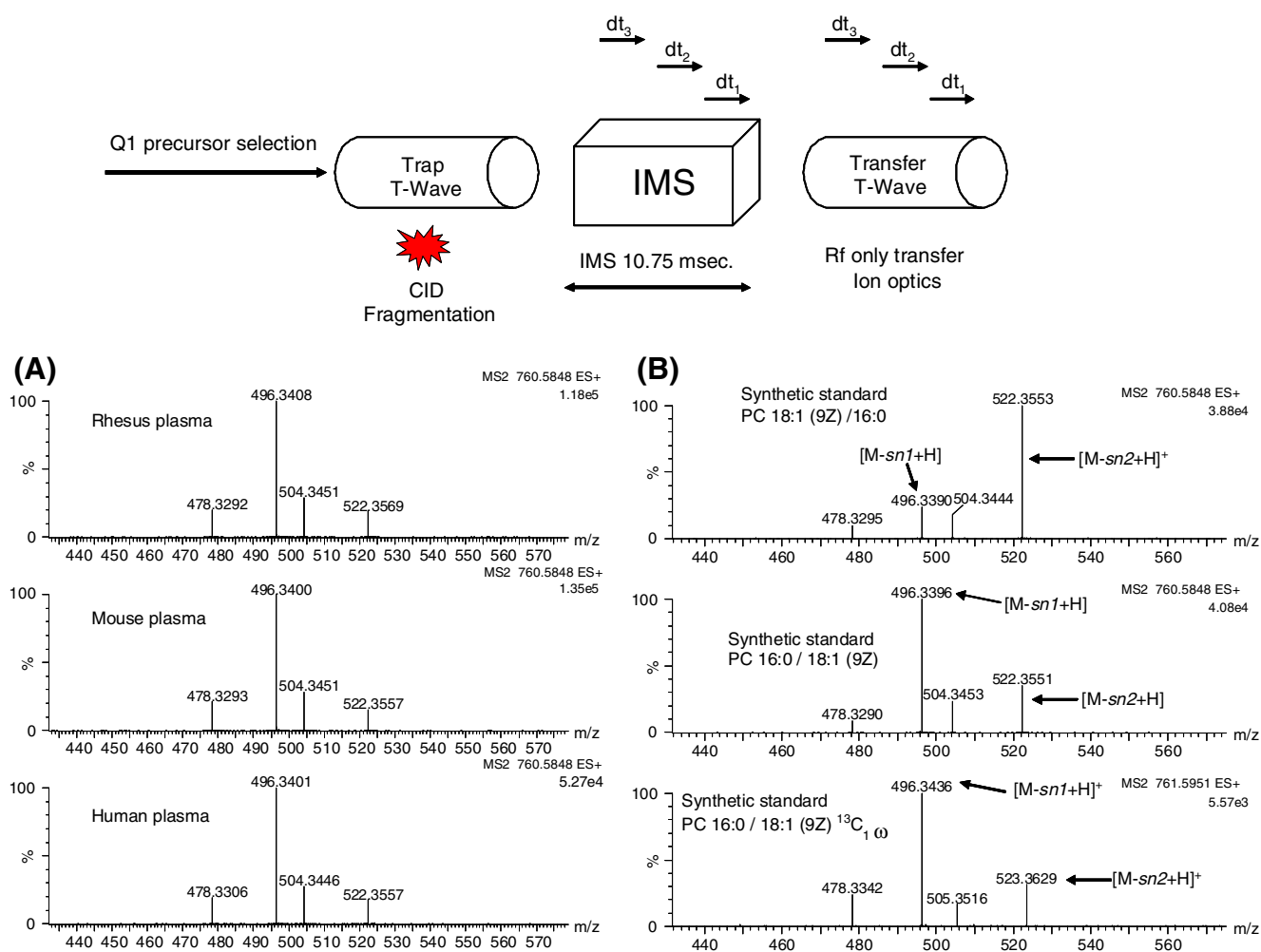


**Figure 3.** Localization of fatty acyl substituent in phosphatidylcholines; PC 16:0/18:1 (9Z) fragmentation was conducted by selecting the ion at  $m/z$  760.5 in the quadrupole region Q1 followed by collision-induced fragmentation in the trap region. **(A)** Shows the  $m/z$  430–580 region of collision-induced dissociation mass spectra for drift time regions 2 and 3 for rhesus (upper panel), mouse (mid panel), and human plasma (lower panel) samples by LC-IMS/TOF. **(B)** Depicts the fragmentation pattern for synthetic standards PC 16:0/18:1 (9Z) (upper panel), PC 18:1 (9Z)/16:0 (mid panel), and PC 16:0/18:1 (9Z) ( $^{13}C_1$  in  $\omega$  methyl position) (lower panel) in drift time regions 2 and 3 by flow injection analysis.  $dt$ =drift time for fragment ions generated in the trap region

impurities, as in the vast majority of cases, in-vivo *sn-1* fatty acyl moieties are saturated [44]. This observation has been previously noted by Ekroos et al. [45], in which in their analysis synthetic standards were found to contain ~15% isomeric impurities by enzymatic means and mass spectrometry as described in the introduction section of this manuscript. In contrast to this, where the purity (~97%) was known for the synthetic “ $^{13}C_1$  labeled” standard, the loss of *sn-1* [ $m/z$  522 or  $m/z$  523 (labeled synthetic standard)] relative to *sn-2* ( $m/z$  496) was ~26% for all plasma samples and ~31% for the labeled synthetic standard. If one takes into account the natural isotopic abundance of the  $^{13}C_1$  isotope, the percentage corresponds to ~29.9%, therefore ~3.9% higher than the plasma samples, this is in close correlation with the purity value provided to us by the supplier of the labeled standard. Due to the fact that this ratio was confirmed with the labeled sample (with known purity) and in none of the spectra where

the human, rhesus, or mouse plasma depicted in Figure 3a showed the ratio for the loss of *sn-1* relative to *sn-2* higher than the labeled synthetic standard, one can assume with a certain degree of confidence that indeed the plasma samples had negligible or no isomeric combinations, which (1) could affect the fatty acyl localization, and (2) impede localization of the double bond. Even for synthetic standards that contain ~12% impurity, it was possible to localize the double bond in the fatty acyl chain as described later on in the manuscript. This particular finding leads to the postulation that it is possible to predict the location of the fatty acyl groups on the basis of the intensity ratios between the different losses of the fatty acyl moieties. The observation that the  $[M - sn2 + H]^+$  ions are most abundant may well be due to the tertiary  $\alpha$ -hydrogen atom, which can form a hydrogen bond with the carbonyl oxygen of the *sn-1* group and thus may hinder the formation of the  $[M - sn1 + H]^+$  ions.

### Location of the Double Bond Position in the Fatty Acyl Substituent

The data generated from the drift time region 4 shows clear isolation in the drift tube of the ion that contains the M-phosphoryl choline  $m/z$  577 (Figures 1c and 2c). This fragment ion gives rise to the formation of the acylium ions (Figure 5a) corresponding to FA 18:1 (9Z) ( $sn$ -2-CO<sup>+</sup>) with  $m/z$  265.2533 (+0.8 ppm) and FA 16:0 ( $sn$ 1-CO<sup>+</sup>) with  $m/z$  239.2380 (+2.1 ppm) as visualized in Scheme 2 by sequences **b**→**c** and **b**→**d** → **e**. These acylium ions eliminate a molecule of water to give the ions  $m/z$  247 and 221 respectively. In Scheme 3, a mechanism is proposed for the loss of water from ion **c** with  $m/z$  265. It involves a successive 1,5-hydride shift from the C5 methylene group to the carbonyl carbon atom, a proton abstraction by the carbonyl oxygen from the C4 methylene group, a 1,3-hydride shift from the C3 methylene group to the carbonyl carbon atom, and a proton abstraction from the C2 methylene group by the generated hydroxyl group, as visualized by the sequence **c**→**f**→**g**→**h**→**i**. Ion **i** can then eliminate by heterolytic cleavage a water molecule to give ion **j** with  $m/z$  247. The latter ion thus contains at its original carbonyl end a delocalized pentadienyl cation moiety being consistent with the presence of a relatively abundant ion at  $m/z$  67 having the elemental composition of C<sub>5</sub>H<sub>7</sub> (see Table S-1, section 4) that can be formed by a 1,2-elimination reaction from ion **j** to give ion **k** (see Scheme 3). In a similar way a molecule of water can be eliminated from ion **e** with  $m/z$  239 (see Scheme 2) to give the ion with  $m/z$  221 that can generate by a 1,2-elimination reaction the C<sub>5</sub>H<sub>7</sub><sup>+</sup> ion **k** with  $m/z$  67 as well.

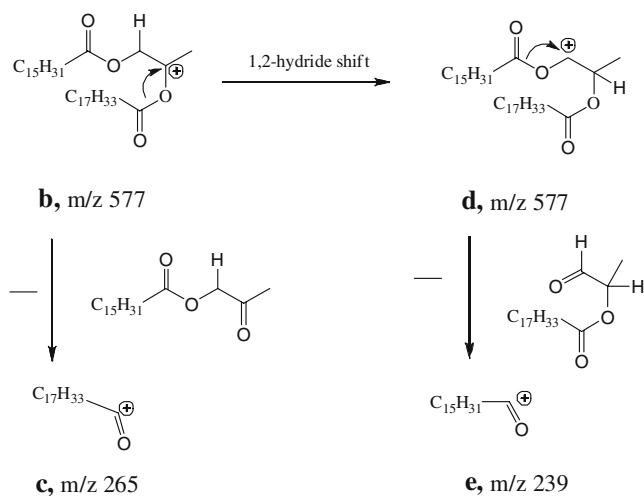
At this point, it should be noted that the most abundant hydrocarbon fragment ions as observed in Figure 4a also have two double bonds, indicating that the dehydrated acylium ions C<sub>16</sub>H<sub>29</sub><sup>+</sup> and C<sub>18</sub>H<sub>33</sub><sup>+</sup> are the key precursor ions for their formation (note that Figure 4a refers to PC

16:0/18:0 having two saturated fatty acid groups). A very interesting and important observation is made comparing the C<sub>5</sub>H<sub>7</sub><sup>+</sup> ion to its higher homologues. It can be seen that from C<sub>9</sub> containing ions onwards the hydrocarbon fragments not only possess two double bonds, but also three double bonds. The latter must originate from the FA 18:1(9Z) chain, and the fact that C<sub>9</sub>H<sub>13</sub><sup>+</sup> is the first ion having three double bonds is in perfect agreement with the double bond at position 9 of the fatty acid chain  $sn$ -2 (Figure 4b), irrespective of the pathway of its formation. Such location of the double bond is also possible with an increased level of unsaturation as in the case of PC 16:0/18:2 (9Z, 12Z). This is shown by the spectrum in Figure 4c, where the C<sub>5</sub> to C<sub>8</sub> containing ions have two double bonds, the C<sub>9</sub> to C<sub>11</sub> containing ions have three double bonds, and the C<sub>12</sub> and higher homologue ions have four double bonds. This is again in perfect agreement with the double bonds at positions 9 and 12 of the fatty acid chain  $sn$ -2. Figure 4d shows the fragmentation of human plasma sample for PC 16:0/18:1 (9Z) from the same drift time region as the Figure 4 synthetic standards. As observed, it is shown that it is possible to localize the double bond position not only in synthetic standards but also in biological samples with on-line LC coupled with IMS-TOF.

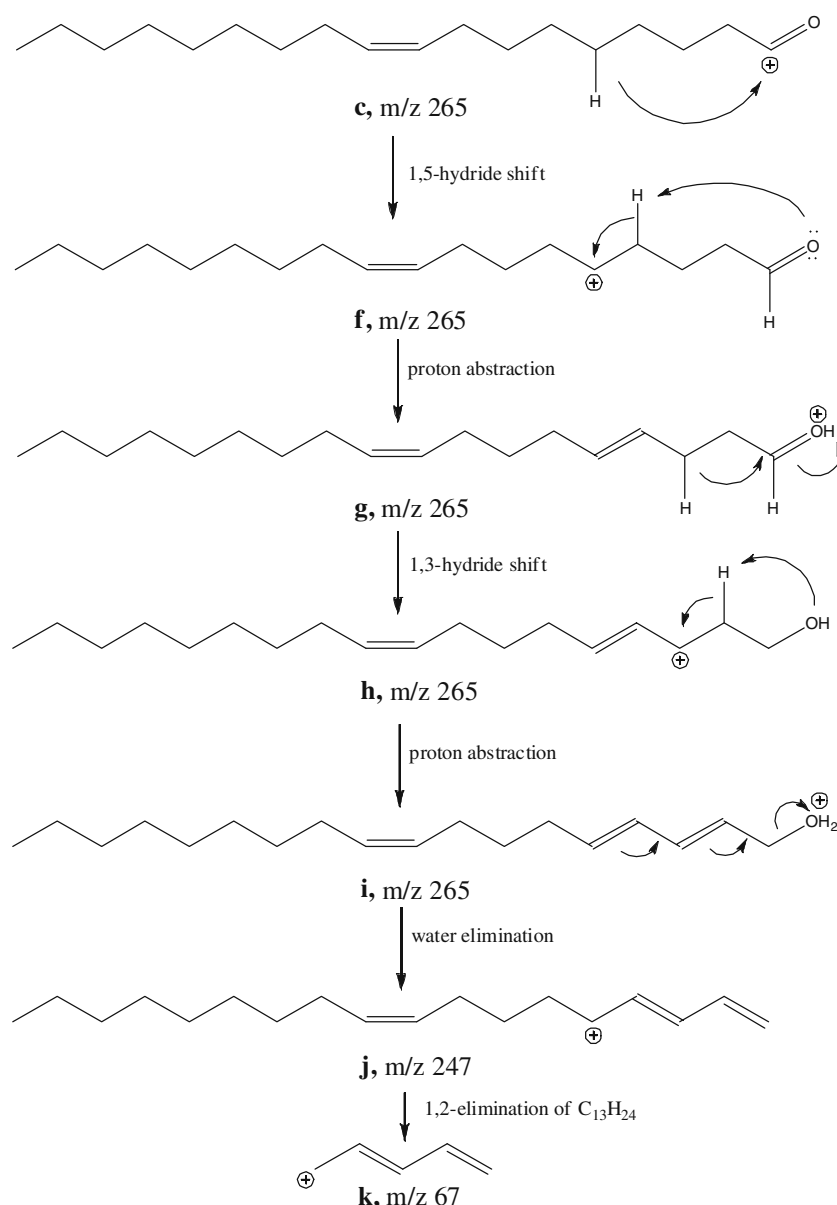
In order to prove that the double bond localization can be attained in either the  $sn$ -1 or  $sn$ -2 position, synthetic standards were utilized [PC 16:0/18:1 (9Z) and PC 18:1 (9Z)/16:0]. Figure S-3 in the supplementary section shows the diagnostic fragment ion  $m/z$  121, which corresponds to the fatty acyl chain containing the double bond position as already observed in Figure 4B, therefore proving that it is certainly possible to localize the double bond position irrespective of fatty acyl localization.

Research has been recently undertaken [22] to locate the double bond in long chain unsaturated fatty acids using of a lithium adduct and a linear ion trap mass spectrometer. The majority of the fragment ions generated in that work arose from  $\beta$ -cleavage with a  $\gamma$ -H shift via a McLafferty-type of rearrangement [46]. Although that research yielded an important set of information, this was conducted using a simpler and less complex system by flow injection analysis infusion with free fatty acids standards. In contrast, in the present study it has been demonstrated that hydrocarbon ions from the fatty acyl chains using the ion mobility set-up can be relatively easily generated and that they were of general high abundance for performing accurate mass measurements, which in itself was key to postulate the fragmentation mechanism described here.

It is well known that unsaturated hydrocarbon ions may suffer from hydrogen and skeletal rearrangements. It is therefore surprising that in the present research, double bond location in the fatty acid chain, discussed above, can be easily derived from the spectra. One reason may be that the proposed dehydrated acylium ions have a highly resonance-stabilized pentadienyl cation moiety that on energetic grounds prevent hydrogen and skeletal rearrangements to



Scheme 2. Formation of the acylium ions C<sub>17</sub>H<sub>33</sub>CO<sup>+</sup> with  $m/z$  265 and C<sub>15</sub>H<sub>31</sub>CO<sup>+</sup> with  $m/z$  239 from the M-phosphoryl choline ion  $m/z$  577

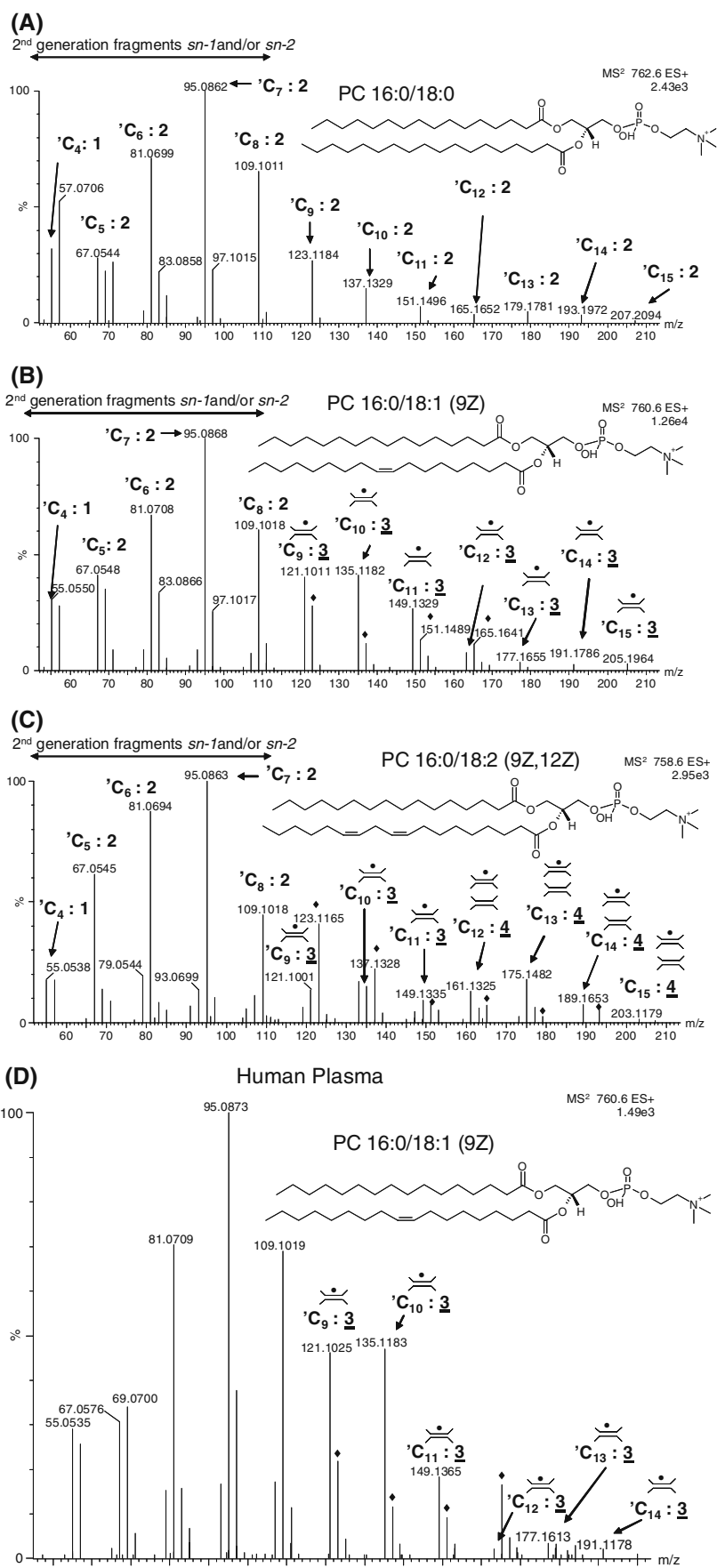


**Scheme 3.** Proposed mechanism for the loss of water from the acylium ion with  $m/z$  265 and one of its further fragmentations to give the hydrocarbon ion  $C_5H_7^+$  with  $m/z$  67

occur. Yet, in Table S-1 and Figure 4, the saturated  $C_4H_9^+$  ion with a notable abundance is present. This prompted us to study PC [16:0/18:1 (9Z)] specifically labeled with  $^{13}C$  at the terminal methyl group of the *sn*-2 fatty acid chain in order to find out which hydrocarbon ion fragments contain  $^{13}C$  and, thus, whether also fragmentation from the  $\omega$  end might take place. The spectra of the unlabeled and  $^{13}C$ -labeled compound are given in Figure 5a and b, respectively. Apart from the peaks at  $m/z$  266.2554 ( $-4.1$  ppm,  $^{13}C_1^{12}C_{18}H_{33}O$ ) and  $m/z$  248.2455 ( $+1.6$  ppm,  $^{13}C_1^{12}C_{18}H_{31}$ ) in Figure 5b, which are due to the  $^{13}C$ -labeled acylium ion and its dehydrated fragment ion from the *sn*-2 fatty acid chain, the peaks denoted with an asterisk in the lower mass region correspond to hydrocarbon ions containing the  $^{13}C$ -label. These peaks have a

low intensity and from comparison of Figure 5b with Figure 5a it may be concluded that the majority of the hydrocarbon ions are

**Figure 4.** (A) Synthetic standard second generation fragment ions region 4 for PC (16:0/18:0) by flow injection TAP analysis. (B) Synthetic standard second generation fragment ions region 4 for PC [16:0/18:1(9Z)] by flow injection TAP analysis. (C) Synthetic standard second generation fragment ions region 4 for PC [16:0/18:2(9Z, 12Z)] by flow injection TAP analysis. (D) Human plasma second generation fragment ions region 4 for PC [16:0/18:1(9Z)] by LC-IMS/TOF TAP analysis. Fragment ions that belongs to either *sn*-1 or *sn*-2 fatty acyl chain are denoted by a filled circle for FA 18:1 (9Z) or FA 18:1 (9Z, 12Z)-containing and filled diamond for FA 16:0-containing



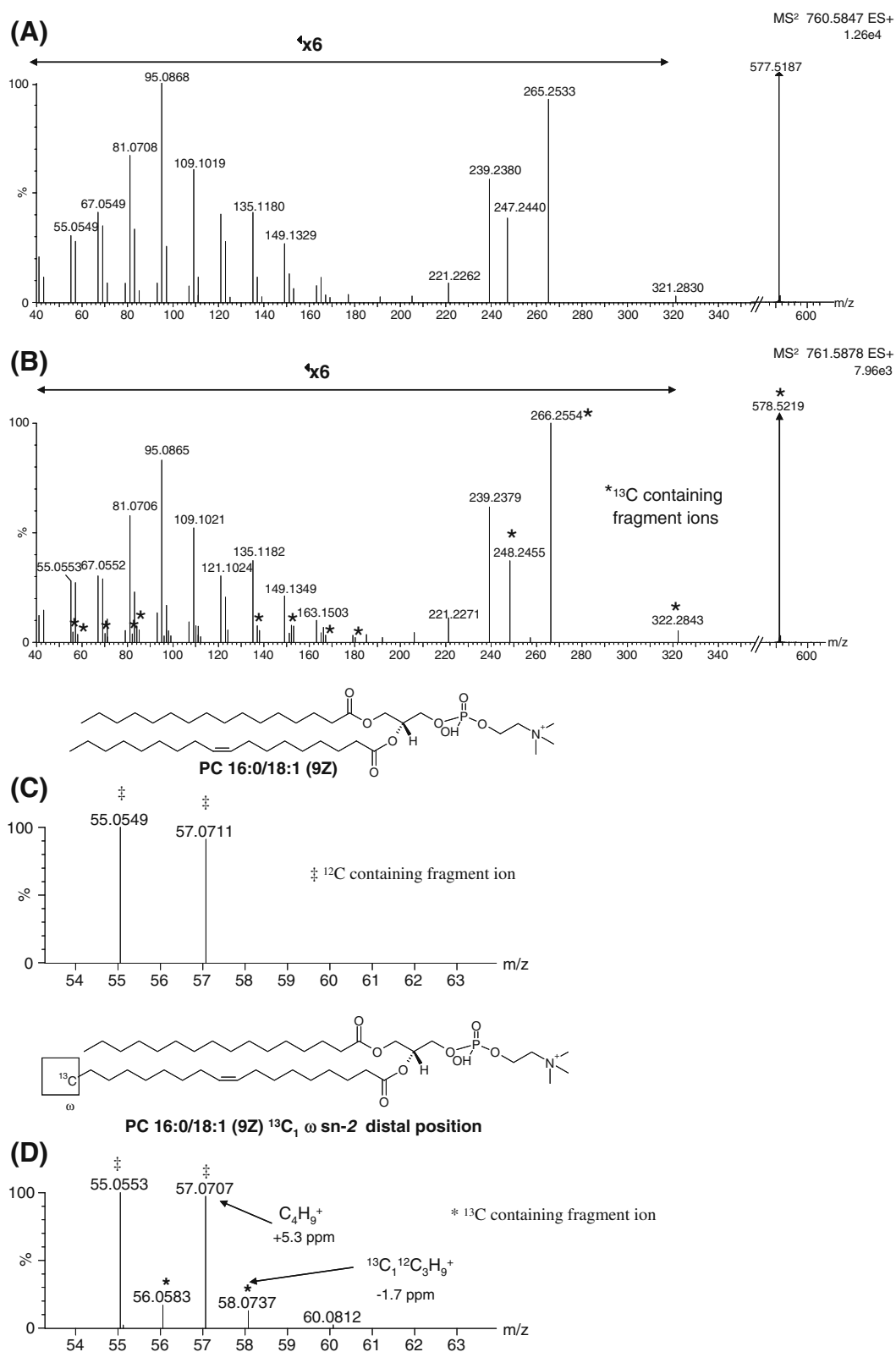


**Figure 5.** Fragment ion spectra from region 4 using the unlabeled synthetic version of PC [16:0/18:1(9Z)] and the synthetic stable isotopic labeled  $^{13}\text{C}$  in the  $\omega$  terminal position by flow injection TAP analysis. **(A)** Unlabeled second generation of fragment ions region 4 for PC [16:0/18:1(9Z)]. **(B)** Stable isotope  $^{13}\text{C}$  labeled second generation of fragment ions region 4 for PC [16:0/18:1(9Z)]. **(C)** Unlabeled second generation of fragment ions region 4 for PC [16:0/18:1(9Z)] showing zoomed region for lower mass range. **(D)** Stable isotope  $^{13}\text{C}$  labeled second generation of fragment ions region 4 for PC [16:0/18:1(9Z)] showing zoomed region for lower mass range



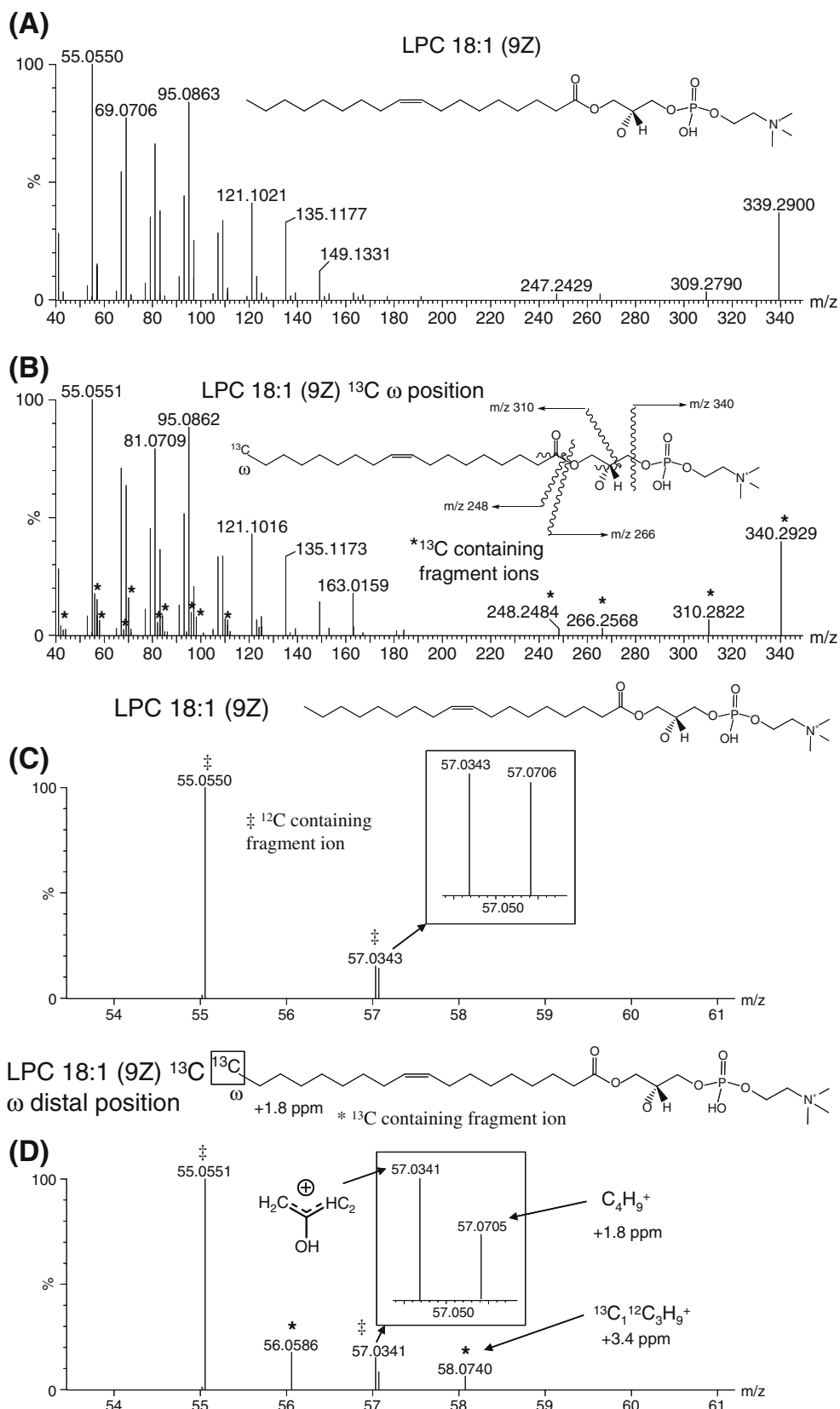


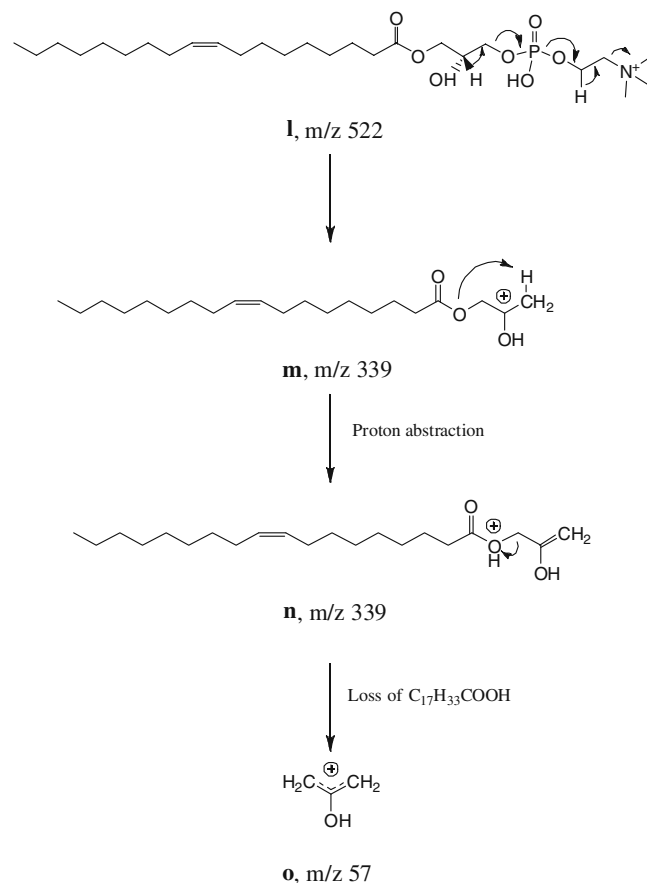
**Figure 6.** Fragment ion spectra from region 2 using the unlabeled version of LPC 18:1(9Z) and the stable isotopic labeled  $^{13}\text{C}$  in the  $\omega$  terminal position by flow injection TAP analysis. **(A)** Unlabeled second generation of fragment ions region 2 for LPC 18:1(9Z). **(B)** Stable isotope  $^{13}\text{C}$  labeled second generation of fragment ions region 2 for LPC 18:1(9Z). **(C)** Unlabeled second generation of fragment ions region 2 for LPC 18:1(9Z) showing zoomed region for lower mass range. **(D)** Stable isotope  $^{13}\text{C}$  labeled second generation of fragment ions region 2 for LPC 18:1(9Z) showing zoomed region for lower mass range

generated from the dehydrated acylium ions by elimination of neutrals containing the  $^{13}\text{C}$ -label. It is not clear how the low abundant  $^{13}\text{C}$  containing hydrocarbon ions are formed, but if a small fraction of the dehydrated acylium ions would eliminate the pentadienyl moiety as a neutral, for example as 1,3,5-hexatriene, the resulting hydrocarbon fragment ion may undergo skeletal rearrangements prior to fragmentation. This would lead to scrambling of the carbon atoms, and indeed Figure 5b shows that the peaks at  $m/z$  55 ( $\text{C}_4\text{H}_7^+$ ) and  $m/z$  57 ( $\text{C}_4\text{H}_9^+$ ) of spectrum Figure 5a have only shifted to a minor extent to  $m/z$  56 ( $^{13}\text{C}_1\text{C}_3\text{H}_7^+$ ) and  $m/z$  58 ( $^{13}\text{C}_1\text{C}_3\text{H}_9^+$ ); see also the corresponding zoomed regions in the spectra Figure 5c and d.

A further study was performed by using LPC 18:1 (9Z), labeled with  $^{13}\text{C}$  in the terminal  $\omega$ -methyl group and having only one fatty acid chain. Figure 6a depicts the fragmentation of LPC 18:1 (9Z) under TAP conditions. The  $^{13}\text{C}$  label was retained in the hydrocarbon fragment ions until the 'C8 position (Table S-2) and then it was only present in the dehydrated acylium ion  $m/z$  248.2568 ( $^{12}\text{C}_{17}^{13}\text{C}_1\text{H}_{31}$ , 10.1 ppm), the acylium ion  $m/z$  266.2568 ( $^{12}\text{C}_{17}^{13}\text{C}_1\text{H}_{33}\text{O}$ , +1.1 ppm), and the ions with  $m/z$  310.2929 ( $^{12}\text{C}_{19}^{13}\text{C}_1\text{H}_{37}\text{O}_2$ , -1.6 ppm) and  $m/z$  340.2929 ( $^{12}\text{C}_{20}^{13}\text{C}_1\text{H}_{39}\text{O}_3$ , -1.2 ppm) (Figure 6b). Interestingly, further inspection of the lower mass range revealed the presence of two fragment ions;  $m/z$  57.0341 (+1.8 ppm,  $\text{C}_3\text{H}_5\text{O}$ ) and  $m/z$  57.0705 (+1.8 ppm  $\text{C}_4\text{H}_9$ ) (Figure 6c and d). The mass spectral resolution was sufficient to mass resolve these two fragment ions, which were 36.4 mDa apart. These two ions were only observed for the LPC, and a more detailed mechanistic scheme for the formation of the ion with  $m/z$  57.0341 is proposed in Scheme 4 as sequence  $\mathbf{l} \rightarrow \mathbf{m} \rightarrow \mathbf{n} \rightarrow \mathbf{o}$ , where the first step is similar to sequence  $\mathbf{a} \rightarrow \mathbf{b}$  in Scheme 1 and where ion  $\mathbf{o}$  is a resonance stabilized 2-hydroxy-allyl cation. As in the case of PC [16:0/18:1 (9Z)], the ion at  $m/z$  57.0705 shifts only partly to  $m/z$  58.0740 ( $^{13}\text{C}_1^{12}\text{C}_3\text{H}_9$ , +3.4 ppm) upon  $^{13}\text{C}$ -labeling indicating the occurrence of carbon skeletal rearrangements as noted before. Nevertheless, the majority of the hydrocarbon fragment ions originate from the dehydrated acylium ions by elimination of neutrals containing the  $^{13}\text{C}$ -label, and again it is equally well possible to locate the double bond position in the LPC lipid classes as shown above for the PC lipid classes.

## Conclusion

A faster, selective, and a more straightforward approach was employed in this study for the comprehensive fragmentation of PCs either by flow injection analysis-IMS/TOF using synthetic standards or by LC-IMS/TOF using plasma from different species (human, rhesus, and mouse). The use of TAP fragmentation together with ion mobility separation of fragment ions enabled the localization of the fatty acyl positions and double bonds in PCs and LPCs. The capability to generate fragment ion information concerning the *sn*-1 and *sn*-2 positions of the



Scheme 4. Proposed mechanism for the formation of the fragment ion  $\text{C}_3\text{H}_5\text{O}^+$  ion with  $m/z$  57.0341 arising from the TAP fragmentation of LPC 18:1(9Z)

fatty acyl substituents has streamlined our identification process and minimized the need for time-consuming enzymatic assays to determine *sn*-1 and *sn*-2 fatty acyl substituent positions. The method described in this study has the advantage to speed up the analysis and simplify the identification process via enhanced fragmentation in combination with accurate mass.

This study is an extension of the investigations initiated by other researchers [12–14, 17, 18, 20, 22, 47, 48]. The observations in the current study recapitulate and further validate previous findings obtained either by the use of alkali metal adducts (lithium or sodium) in positive ion, or by the use of negative ion FAB. Nonetheless, the main difference is the use of a different mass analyzer, which allowed for accurate mass confirmation of the fragment ions and provided an extra level of selectivity by the application of high-resolution accurate mass ion mobility time-of-flight mass spectrometry. Additionally, hydrocarbon fragmentation data were generated by protonated PCs and LPCs, which aided in the subsequent localization of double bonds.

In our particular context, a more straightforward approach was utilized in which not only qualitative information was obtained but also applicable to quantitative information. Analysis of plasma samples for lipid analysis is already a

complicated affair due to the myriad number of lipids present in the sample. Adding another variable to the analysis, such as introduction post-column of an alkali metal to generate ions like Li<sup>+</sup> adduct ions will further complicate the detection and identification process of an already challenging analysis. Even though volatile lithium salts can be utilized to obtain fatty acyl and double bond position, there is always the risk of unwanted ion source block contamination occurring from prolonged usage. This can pose difficulties in the routine operation of a laboratory such as ours in which a large number of metabolite profiling samples (>1000 per week) measuring different analytes (lipids, bile acids, amino acids, sugars, polar metabolites, etc.) are analyzed. Furthermore, in the strategy described in this study, lower molecular weight species were observed in Figure 6 (*m/z* 57 Scheme 4) generated by TAP fragmentation from the LPC 18:1 (9Z), showing that there are two fragment ions with different elemental compositions that have not been described before. Accurate mass measurement and high-resolution ion mobility permitted this observation.

Extension of this methodology may be applied to other phospholipid classes, and this will be the subject of future research. Besides this, ion mobility added an extra level of selectivity, not only in the MS<sup>2</sup> mode but also in full scan MS because it has provided additional descriptors, such as drift time information besides *m/z*, chromatographic retention time, peak intensity, and peak area.

In summary, it has been possible to analyze biological samples such as plasma for lipid analysis and to obtain structural information in this way. Our methodology and results thus pave the way for precise characterization of lipid profiles in our future studies of various disease models and potential therapies for dyslipidemia and atherosclerosis.

## Acknowledgments

The authors thank Mahsut Ablatt, Dan Xie, and John P. Shockcor for the helpful discussions on the research described in this manuscript.

## Open Access

This article is distributed under the terms of the Creative Commons Attribution Noncommercial License which permits any noncommercial use, distribution, and reproduction in any medium, provided the original author(s) and source are credited.

## References

- Brown, H.A.: Lipidomics and bioactive lipids: specialized analytical methods and lipids in disease. *Preface. Methods Enzymol* **433**, XV–XVI (2007)
- Astarita, G., Ahmed, F., Piomelli, D.: Lipidomic analysis of biological samples by liquid chromatography coupled to mass spectrometry. *Methods Mol. Biol.* **579**, 201–219 (2009)
- Gross, R.W., Jenkins, C.M., Yang, J., Mancuso, D.J., Han, X.: Functional lipidomics: The roles of specialized lipids and lipid-protein interactions in modulating neuronal function. *Prostaglandins Other Lipid Mediat.* **77**, 52–64 (2005)
- Gross, R.W., Han, X.: Lipidomics in diabetes and the metabolic syndrome. *Methods Enzymol* **433**, 73–90 (2007)
- German, J.B., Gillies, L.A., Smilowitz, J.T., Zivkovic, A.M., Watkins, S.M.: Lipidomics and lipid profiling in metabolomics. *Curr. Opin. Lipidol.* **18**, 66–71 (2007)
- Fahy, E., Subramaniam, S., Murphy, R.C., Nishijima, M., Raetz, C.R., Shimizu, T., Spener, F., van Meer, G., Wakelam, M.J., Dennis, E.A.: Update of the LIPID MAPS comprehensive classification system for lipids. *J. Lipid Res.* **50**(Suppl), S9–14 (2009)
- Fahy, E., Subramaniam, S., Brown, H.A., Glass, C.K., Merrill Jr., A.H., Murphy, R.C., Raetz, C.R., Russell, D.W., Seyama, Y., Shaw, W., Shimizu, T., Spener, F., van Meer, G., VanNieuwenhze, M.S., White, S. H., Witztum, J.L., Dennis, E.A.: A comprehensive classification system for lipids. *J. Lipid Res.* **46**, 839–861 (2005)
- Yasuda, T., Ishida, T., Rader, D. J.: Update on the role of endothelial lipase in high-density lipoprotein metabolism, reverse cholesterol transport, and atherosclerosis. *Circ. J.* **74**, 2263–2270 (2010)
- Angell, R., Mitsuhashi, Y., Bigley, K., Bauer, J.E.: Plasma LCAT activity and lipid subfraction composition in obese beagles undergoing weight loss. *Lipids* **44**, 415–424 (2009)
- Griffiths, W.J.: Tandem mass spectrometry in the study of fatty acids, bile acids, and steroids. *Mass Spectrom. Rev.* **22**, 81–152 (2003)
- Pittenauer, E., Allmaier, G.: The renaissance of high-energy CID for structural elucidation of complex lipids: MALDI-TOF/RTOF-MS of alkali cationized triacylglycerols. *J. Am. Soc. Mass Spectrom.* **20**, 1037–1107 (2009)
- Tomer, K.B., Crow, F.W., Gross, M.L.: Location of double-bond position in unsaturated fatty acids by negative ion MS/MS. *J. Am. Chem. Soc.* **105**, 5487–5488 (1983)
- Jensen, N.J., Tomer, K.B., Gross, M.L.: Fast atom bombardment and tandem mass spectrometry of phosphatidylserine and phosphatidylcholine. *Lipids* **21**, 580–588 (1986)
- Jensen, N.J., Tomer, K.B., Gross, M.L.: FAB MS/MS for phosphatidylinositol, -glycerol, -ethanolamine, and other complex phospholipids. *Lipids* **22**, 480–489 (1987)
- Murphy, R.C., Fiedler, J., Hevko, J.: Analysis of nonvolatile lipids by mass spectrometry. *Chem. Rev.* **101**, 479–526 (2001)
- Kerwin, J.L., Tuininga, A.R., Ericsson, L.H.: Identification of molecular species of glycerophospholipids and sphingomyelin using electrospray mass spectrometry. *J. Lipid Res.* **35**, 1102–1114 (1994)
- Murphy, R.C., Harrison, K.A.: Fast atom bombardment mass spectrometry of phospholipids. *Mass Spectrom. Rev.* **13**, 57–75 (1994)
- Pulfer, M., Murphy, R.C.: Electrospray mass spectrometry of phospholipids. *Mass Spectrom. Rev.* **22**, 332–364 (2003)
- Hsu, F.F., Turk, J.: Structural characterization of unsaturated glycerophospholipids by multiple-stage linear ion-trap mass spectrometry with electrospray ionization. *J. Am. Soc. Mass Spectrom.* **19**, 1681–1691 (2008)
- Hsu, F.F., Turk, J.: Electrospray ionization/tandem quadrupole mass spectrometric studies on phosphatidylcholines: The fragmentation processes. *J. Am. Soc. Mass Spectrom.* **14**, 352–363 (2003)
- Bryant, D.K., Orlando, R.C., Fenselau, C., Sowder, R.C., Henderson, L. E.: Four-sector tandem mass spectrometric analysis of complex mixtures of phosphatidylcholines present in a human immunodeficiency virus preparation. *Anal. Chem.* **63**, 1110–1114 (1991)
- Hsu, F.F., Turk, J.: Elucidation of the double-bond position of long-chain unsaturated fatty acids by multiple-stage linear ion-trap mass spectrometry with electrospray ionization. *J. Am. Soc. Mass Spectrom.* **19**, 1673–1680 (2008)
- Thomas, M.C., Mitchell, T.W., Blanksby, S.J.: Ozonolysis of phospholipid double bonds during electrospray ionization: A new tool for structure determination. *J. Am. Chem. Soc.* **128**, 58–59 (2006)
- Thomas, M.C., Mitchell, T.W., Harman, D.G., Deeley, J.M., Murphy, R.C., Blanksby, S.J.: Elucidation of double bond position in unsaturated lipids by ozone electrospray ionization mass spectrometry. *Anal. Chem.* **79**, 5013–5022 (2007)
- Thomas, M.C., Mitchell, T.W., Harman, D.G., Deeley, J.M., Nealon, J. R., Blanksby, S.J.: Ozone-induced dissociation: elucidation of double bond position within mass-selected lipid ions. *Anal. Chem.* **80**, 303–311 (2008)

26. Becker, C., Fernandez-Lima, F.A., Gillig, K.J., Russell, W.K., Cologna, S.M., Russell, D.H.: A novel approach to collision-induced dissociation (CID) for ion mobility-mass spectrometry experiments. *J. Am. Soc. Mass Spectrom.* **20**, 907–914 (2009)
27. Belov, M.E., Buschbach, M.A., Prior, D.C., Tang, K., Smith, R.D.: Multiplexed ion mobility spectrometry-orthogonal time-of-flight mass spectrometry. *Anal. Chem.* **79**, 2451–2462 (2007)
28. Fenn, L.S., Kliman, M., Mahsut, A., Zhao, S.R., McLean, J.A.: Characterizing ion mobility-mass spectrometry conformation space for the analysis of complex biological samples. *Anal. Bioanal. Chem.* **394**, 235–244 (2009)
29. Fenn, L.S., McLean, J.A.: Biomolecular structural separations by ion mobility-mass spectrometry. *Anal. Bioanal. Chem.* **391**, 905–909 (2008)
30. Hill, H.H., Siems, W.F., Stlouis, R.H., Mcminn, D.G.: Ion Mobility Spectrometry. *Anal. Chem.* **62**, A1201–A1209 (1990)
31. Guo, Y., Ling, Y., Thomson, B.A., Siu, K.W.: Combined ion-mobility and mass-spectrometry investigations of metallothionein complexes using a tandem mass spectrometer with a segmented second quadrupole. *J. Am. Soc. Mass Spectrom.* **16**, 1787–1794 (2005)
32. Ruotolo, B.T., Gillig, K.J., Stone, E.G., Russell, D.H.: Peak capacity of ion mobility mass spectrometry: separation of peptides in helium buffer gas. *J. Chromatogr. B Analyt. Technol. Biomed. Life Sci* **782**, 385–392 (2002)
33. Trimpin, S., Clemmer, D.E., McEwen, C.N.: Charge-remote fragmentation of lithiated fatty acids on a TOF-TOF instrument using matrix-ionization. *J. Am. Soc. Mass Spectrom.* **18**, 1967–1972 (2007)
34. Zhu, M., Bendiak, B., Clowers, B., Hill Jr., H.H.: Ion mobility-mass spectrometry analysis of isomeric carbohydrate precursor ions. *Anal. Bioanal. Chem.* **394**, 1853–1867 (2009)
35. Ruotolo, B.T., McLean, J.A., Gillig, K.J., Russell, D.H.: Evidence for macromolecular protein rings in the absence of bulk water. *Science* **310**, 1658–1661 (2005)
36. Ruotolo, B.T., Hyung, S.J., Robinson, P.M., Giles, K., Bateman, R.H., Robinson, C.V.: Ion mobility-mass spectrometry reveals long-lived, unfolded intermediates in the dissociation of protein complexes. *Angew. Chem. Int. Ed. Engl.* **46**, 8001–8004 (2007)
37. Smith, D.P., Knapman, T.W., Campuzano, I., Malham, R.W., Berryman, J.T., Radford, S.E., Ashcroft, A.E.: Deciphering drift time measurements from travelling wave ion mobility spectrometry-mass spectrometry studies. *Eur. J. Mass Spectrom. (Chichester, Engl)* **15**, 113–130 (2009)
38. Williams, J.P., Lough, J.A., Campuzano, I., Richardson, K., Sadler, P. J.: Use of ion mobility mass spectrometry and a collision cross-section algorithm to study an organometallic ruthenium anticancer complex and its adducts with a DNA oligonucleotide. *Rapid Commun. Mass Spectrom.* **23**, 3563–3569 (2009)
39. Williams, J.P., Bugarcic, T., Habtemariam, A., Giles, K., Campuzano, I., Rodger, P.M., Sadler, P.J.: Isomer Separation and Gas-Phase Configurations of Organoruthenium Anticancer Complexes: Ion Mobility Mass Spectrometry and Modeling. *J. Am. Soc. Mass Spectrom.* **20**, 1119–1122 (2009)
40. Wildgoose, J., McKenna, T., Hughes, C., Giles, K., Pringle, S., Campuzano, I., Langridge, J., Bateman, R.H.: Using a novel traveling wave ion mobility device coupled with a time-of-flight mass spectrometer for the analysis of intact proteins. *Mol. Cell. Proteom.* **5**, S14–S14 (2006)
41. Bligh, E.G., Dyer, W.J.: A rapid method of total lipid extraction and purification. *Can. J. Biochem. Physiol.* **37**, 911–917 (1959)
42. Castro-Perez, J. M., Kamphorst, J., DeGroot, J., Lafeber, F., Goshawk, J., Yu, K., Shockcor, J. P., Vreeken, R. J., Hankemeier, T.: Comprehensive LC-MS<sup>E</sup> lipidomic analysis using a shotgun approach and its application to biomarker detection and identification in osteoarthritis patients. *J. Proteome Res.* **9**, 2377–2389 (2010)
43. Trimpin, S., Tan, B., Bohrer, B.C., O'Dell, D.K., Merenbloom, S.I., Pazos, M.X., Clemmer, D.E., Walker, J.M.: Profiling of phospholipids and related lipid structures using multidimensional ion mobility spectrometry-mass spectrometry. *Int. J. Mass Spectrom.* **287**, 58–69 (2009)
44. Arvidson, G.A.: Biosynthesis of phosphatidylcholines in rat liver. *Eur. J. Biochem.* **5**, 415–421 (1968)
45. Ekroos, K., Ejlsing, C.S., Bahr, U., Karas, M., Simons, K., Shevchenko, A.: Charting molecular composition of phosphatidylcholines by fatty acid scanning and ion trap MS3 fragmentation. *J. Lipid Res.* **44**, 2181–2192 (2003)
46. McLafferty, F.: Mass Spectrometric Analysis: Molecular Rearrangements. *Anal. Chem.* **31**, 82–87 (1959)
47. Hsu, F.F., Bohrer, A., Turk, J.: Formation of lithiated adducts of glycerophosphocholine lipids facilitates their identification by electrospray ionization tandem mass spectrometry. *J. Am. Soc. Mass Spectrom.* **9**, 516–526 (1998)
48. Hsu, F.F., Turk, J.: Distinction among isomeric unsaturated fatty acids as lithiated adducts by electrospray ionization mass spectrometry using low energy collisionally activated dissociation on a triple stage quadrupole instrument. *J. Am. Soc. Mass Spectrom.* **10**, 600–612 (1999)